White organic light-emitting diodes with 4 nm metal electrode

Simone Lenk, Tobias Schwab, Sylvio Schubert, Lars Müller-Meskamp, Karl Leo, Malte C. Gather, and Sebastian Reineke

Citation: Applied Physics Letters **107**, 163302 (2015); doi: 10.1063/1.4934274
View online: http://dx.doi.org/10.1063/1.4934274
View Table of Contents: http://scitation.aip.org/content/aip/journal/apl/107/16?ver=pdfcov
Published by the AIP Publishing

White organic light-emitting diodes with 4 nm metal electrode

Simone Lenk,[1] Tobias Schwab,[1] Sylvio Schubert,[1] Lars Müller-Meskamp,[1] Karl Leo,[1] Malte C. Gather,[1,2] and Sebastian Reineke[1]
[1]*Institut für Angewandte Photophysik, Technische Universität Dresden, George-Bähr-Straße 1, 01069 Dresden, Germany*
[2]*Organic Semiconductor Centre, SUPA, School of Physics and Astronomy, University of St Andrews, North Haugh, St Andrews KY16 9SS, United Kingdom*

(Received 3 July 2015; accepted 9 October 2015; published online 21 October 2015)

We investigate metal layers with a thickness of only a few nanometers as anode replacement for indium tin oxide (ITO) in white organic light-emitting diodes (OLEDs). The ultrathin metal electrodes prove to be an excellent alternative that can, with regard to the angular dependence and efficiency of the OLED devices, outperform the ITO reference. Furthermore, unlike ITO, the thin composite metal electrodes are readily compatible with demanding architectures (e.g., top-emission or transparent OLEDs, device unit stacking, etc.) and flexible substrates. Here, we compare the sheet resistance of both types of electrodes on polyethylene terephthalate for different bending radii. The electrical performance of ITO breaks down at a radius of 10 mm, while the metal electrode remains intact even at radii smaller than 1 mm. © *2015 AIP Publishing LLC*.
[http://dx.doi.org/10.1063/1.4934274]

Flexible or even stretchable optoelectronic and photonic devices such as paper-like displays,[1] lighting,[2] sensors,[3] artificial skin,[4] and bio-integrated electronics[5] set new benchmarks in science and technology. In this context, organic semiconductors are very promising materials due to their inherent softness and their compatibility with facile roll-to-roll processing and printing.

For many years, however, the development of flexible devices was hampered by limitations of the transparent electrode material, which needs to combine high conductivity, excellent transparency, mechanical flexibility (bendable and stretchable), low cost, and electrical compatibility with the semiconducting materials used. To overcome this technological bottleneck, many electrode systems have been studied, including conductive oxides, polymers, carbon nanotube films, graphene films, metal nanostructures, and nanowire networks.[6–11] However, all of these new electrodes struggle to reach the electrical and optical performance of indium tin oxide (ITO)—the *de facto* standard in the field.

Promising results have been achieved in the last 5 years[8,11–13] with alternative electrodes, but none of these has been widely accepted as a replacement for ITO. However, replacing ITO becomes increasingly urgent due to the limited world-wide indium resources. Moreover, ITO and the other aforementioned electrodes can, in most cases, only be used as bottom electrodes. Amongst other issues, this impedes the fabrication of highly transparent devices, which require a transparent electrode to be deposited on top of organic layers and which are essential for a variety of novel applications.

So far, if semi-transparent top-electrodes are to be used in organic light-emitting diodes (OLEDs), silver (Ag) layers of 10–20 nm thickness have typically been used as Ag can be easily evaporated on top of organic layers.[14] Since Ag is known to grow in islands for the first few nanometers, a layer thickness of >10 nm is typically necessary to form a closed and conductive layer. Whilst at this thickness Ag is no longer fully transparent, such thick layers can be advantageous in OLEDs to tune the optical cavity such that light interferes constructively. Monochrome devices with semi-transparent, 21 nm thick Ag top electrodes can exhibit very high efficiencies up to 29%.[15] However, for white emission, light outcoupling needs to be optimized for all colors, and therefore, thinner Ag layers with high transmission over a broad wavelength regime are essential.[16–18]

We have previously demonstrated that a wetting layer comprised of a few nanometers of gold (Au) enables formation of ultrathin Ag electrodes that show excellent performance as top-electrodes of white inverted and non-inverted top-emitting OLEDs, and top-illuminated organic solar cells.[19–21] However, the replacement of the ITO bottom anode by such composite ultrathin electrodes has not been studied before.

In this work, we apply an ultrathin Ag layer as the bottom electrode in a white OLED and compare the performance against a reference device with an ITO electrode. We demonstrate that the ultrathin Ag electrode is a valid alternative to ITO. Furthermore, we investigate bending data of the respective electrodes on polyethylene terephthalate (PET) foil and show that the metal electrode allows significantly smaller bending radii (<1 mm) than ITO.

Figure 1(a) shows the OLED layer structure and electrodes under investigation. The substrate is glass (Corning Eagle XG, Thin Film Devices, Inc.) plus either 90 nm of pre-deposited ITO or an ultrathin metal electrode of 3 nm molybdenum oxide (MoO_3), 2 nm Au, and Ag of different thicknesses. It has been shown previously that MoO_3 and Au assist in the formation of closed Ag layers since the surface energy of Au is greater than that of Ag.[21] Therefore, Ag atoms prefer attaching to the Au surface rather than to each other, which leads to a Frank-van-der-Merwe growth.

The electrode is followed by the organic layers: Spiro-TTB: F6-TCNNQ 2 wt. % (40 nm)/NPD (10 nm)/NPD:Ir(MDQ)2(acac) 10 wt. % (8 nm)/TCTA:Ir(ppy)3 (3 nm)/TCTA:TPBI 2:1 (3 nm)/MADN:TBPe 1 wt. % (10 nm)/BPhen

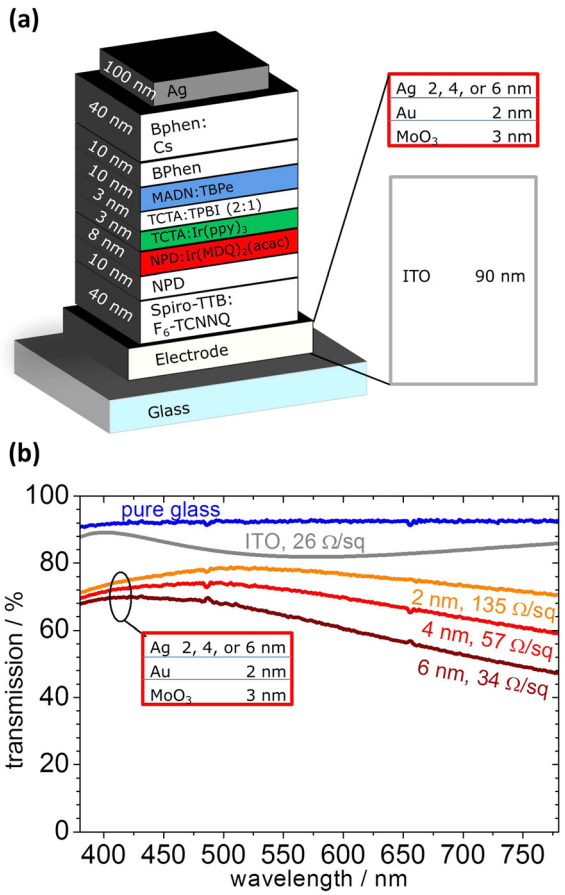

FIG. 1. OLED layer architecture (a) and transmittance of the electrodes with corresponding electrode sheet resistance (b).

(10 nm)/BPhen:Cs (40 nm). An Ag layer (100 nm) is used as cathode. Details about organic materials can be found in Refs. 19 and 22. The thickness of all layers is optimized for maximum device performance of the ITO reference device, and the same thicknesses are used for the OLEDs on the composite electrode. Devices are fabricated in a single chamber vacuum evaporation tool (Kurt J. LESKER & Co.) at a base pressure of 10^{-7} mbar. Immediately after fabrication, all OLEDs are encapsulated with glass lids under nitrogen atmosphere.

PET substrates are purchased from DuPont Teijin Films, USA (Melinex ST 504, 125 μm thick, without a coated planarization layer). Prior to evaporation of the electrodes, the substrates are carefully cleaned with *N*-methyl-2-pyrrolidone, de-ionized water, and ethanol in an ultrasonic bath, and then baked-out at 90 °C under inert nitrogen atmosphere.

Current-voltage (IV) measurements are performed with a KEITHLEY SMU2400 source-measure unit. Luminance (L) is recorded simultaneously with a Si photodiode. The spectral radiance in the forward direction is taken by a calibrated Instrument Systems GmbH CAS140 spectrometer. Transmission is measured using a combined Deuterium and Halogen lamp (AVANTES) and the same spectrometer as for the spectral radiance. The baseline is measured against air. Angular dependent emission is recorded with a custom-built goniometer setup, including a rotation stage and a calibrated fiber coupled spectrometer (OCEAN OPTICS USB4000). External quantum efficiency (EQE) and luminous efficacy (LE) are measured in an Ulbricht sphere (LABSPHERE). Sheet resistance is measured with a four-point-probe measurement stand S 302−4 (LUCASLABS). Roughness measurements are carried out using a Dektak 150 profilometer (VEECO).

All investigated electrodes form conductive layers with high transmission (Fig. 1(b)). The Ag based electrodes reach 60%–80% transmission over the entire visible wavelength regime. Interestingly, even the thinnest composite electrode tested here (2 nm Ag/2 nm Au/3 nm MoO_3) has a sheet resistance of 134 Ω/sq, despite the overall metal layer thickness being just 4 nm.

Figure 2 shows the electrical and optical performance of the OLEDs under investigation. The IVL characteristics are nearly identical for the ITO and the metal electrode (Fig. 2(a)). Only for the device comprising a 2 nm thick Ag layer, the IV curve is slightly flatter, which is related to the higher sheet resistance. Furthermore, the leakage current of the Ag

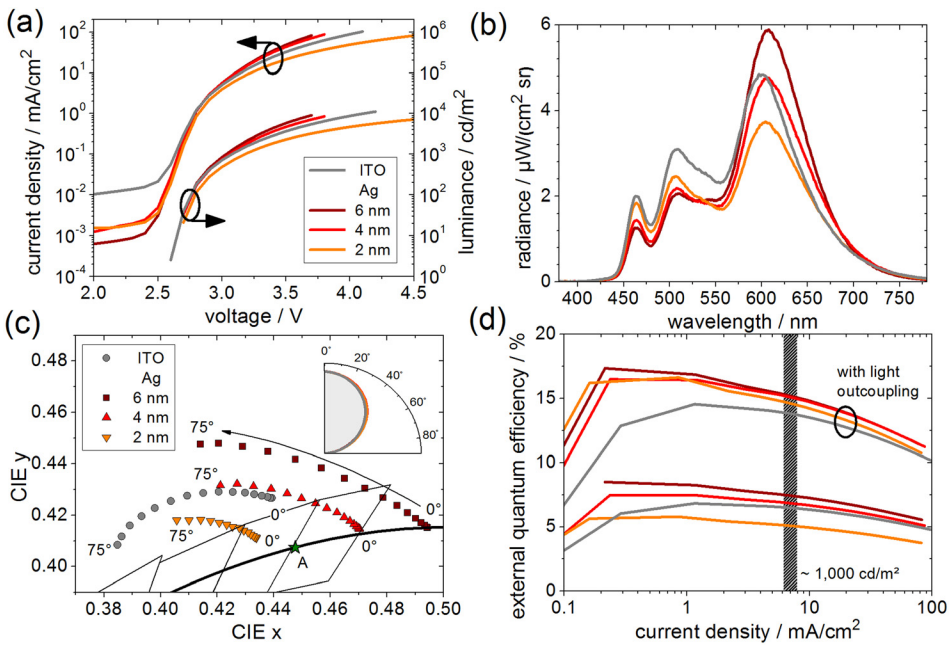

FIG. 2. Performance of white OLEDs with ultrathin metal anodes or ITO anodes (as reference): IVL characteristics (a), spectral emission at a current density of 15 mA/cm^2 (b), angular dependent CIE coordinates at 15 mA/cm^2 in 5° steps and polar diagram (inset) (c), and EQE vs. current density with and without a glass half sphere as light outcoupling structure (d).

TABLE I. OLED performance at 1000 cd/m^2.

Device Type	CIE	CRI	EQE (%)	EQE[a]	LE (lm/W)
ITO	0.436/0.435	84	6.6	2.2×	15.0
Ag					
2 nm	0.433/0.418	86	5.1	2.9×	10.6
4 nm	0.472/0.420	85	6.9	2.2×	16.1
6 nm	0.495/0.423	83	7.5	2.1×	18.3

[a]EQE enhancement when using a glass half sphere for light outcoupling.

based devices is remarkably low. Since all electrodes exhibit a very smooth surface[19–21] and the average roughness is rather similar (<2 nm, see Fig. S1 in the supplementary material[23]), the reason for the relatively high leakage current of the ITO-OLED within this particular run remains unclear.

The spectral emission (Fig. 2(b)) reflects an interesting behavior. In the blue and the green parts of the spectrum, the intensity increases as the Ag layer becomes thinner, which is in good agreement with the transmission data in Fig. 1(b). However, in the red part of the spectrum, the trend is reversed. This can be understood as an effect of the weak optical cavity formed between the electrodes: In the red spectral region, the transmission of the electrode is significantly lower than for blue and green (compare Fig. 1(b)). Like in the case of monochrome devices, the thicker Ag layer forms a stronger cavity (e.g., increases the Purcell effect) for red light and can therefore enhance the emission in a certain wavelength regime.[15,24]

Typically, for OLEDs with thick metal electrodes, the emission color changes strongly with viewing angle—a phenomenon that is undesired in most practical applications.[25]

It is therefore important to investigate the emission at different viewing angles for the white OLEDs containing thin metal electrodes (Fig. 2(c)). The associated spectral radiant intensity is given in the supplementary material[23] (Fig. S2). With increasing Ag thickness, a larger shift of the color coordinates (CIE) is seen due to increasing microcavity effects. However, the OLEDs with ultrathin Ag electrodes have a very weak angular dependence as seen in the strongly magnified CIE diagram in Fig. 2(c). In particular, the OLED with 2 nm Ag shows a significantly smaller color shift (ΔCIE(x,y) = (0.028, −0.007) from 0° to 75°) than the ITO reference device (ΔCIE(x,y) = (0.054, 0.018)). Furthermore, all devices exhibit Lambertian emission characteristics (inset of Fig. 2(c)). In addition, we investigate the CIE color shifts as a function of Ag layer thickness by optical thin film simulations (supplementary material,[23] Fig. S3), yielding good qualitative agreement between simulation and experiment. Figure 2(d) shows the EQE of the OLEDs under investigation with and without a glass half sphere as outcoupling structure. In addition, the performance at a luminance of 1000 cd/m^2 is summarized in Table I.

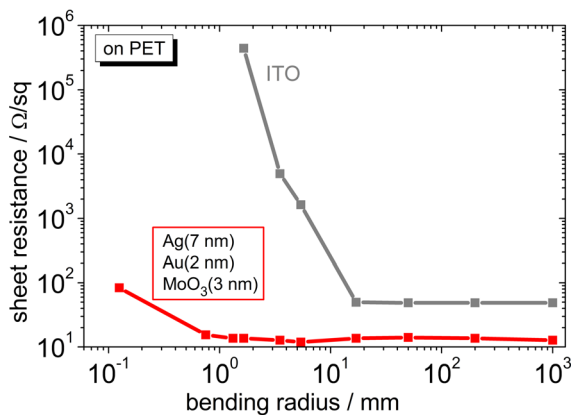

FIG. 3. Cumulative bending test of different electrodes on PET. Electrical functionality of ultrathin Ag electrodes can be achieved for a very small bending radius down to less than 1 mm and 50% strain.

It is worth noting that the OLEDs with 4 and 6 nm Ag layers exhibit a greater EQE than the ITO reference. The same holds for the LE. Furthermore, using the outcoupling half sphere, a very high increase in EQE by a factor of 2.9 is obtained for the sample with 2 nm Ag, indicating that extraction of light trapped in the glass substrate is particularly efficient for this sample. Thus, in terms of performance, our results show that the OLEDs with ultrathin metal electrodes are comparable or even better than OLEDs with ITO anodes. Furthermore, the device lifetime is not influenced by the anode material (see Fig. S4 in the supplementary material[23]).

In order to investigate the bending properties of the anode materials investigated here, we deposited ITO and the composite metal electrode onto a PET substrate, respectively. The sheet resistance for both electrodes after the application of different bending radii is shown in Fig. 3. The ITO electrode maintains useful sheet resistance down to a radius of 10 mm. In contrast, the Ag electrodes remain functional even at a bending radius below 1 mm.

In summary, we have demonstrated that an ultrathin, composite metal electrode can serve as a suitable ITO replacement in white OLEDs due to its high transmission and low sheet resistance. In the future, the metal electrode can be used as both anode and cathode for transparent devices, due to its easy processing and the fact that its deposition does not damage any underlying organic material.[26] Furthermore, bending tests reveal that these electrodes remain highly conductive down to bending-radii of less than 1 mm and 50% strain, by far outperforming the industry-standard ITO. This offers a variety of implementations in non-flat electronics, e.g., conformal device applications, where small bending radii are needed.

[1]J. A. Rogers, Z. Bao, K. Baldwin, A. Dodabalapur, B. Crone, V. R. Raju, V. Kuck, H. Katz, K. Amundson, J. Ewing, and P. Drzaic, Proc. Natl. Acad. Sci. U.S.A. **98**, 4835 (2001).
[2]Z. B. Wang, M. G. Helander, J. Qiu, D. P. Puzzo, M. T. Greiner, Z. M. Hudson, S. Wang, Z. W. Liu, and Z. H. Lu, Nat. Photonics **5**, 753 (2011).
[3]S. C. B. Mannsfeld, B. C.-K. Tee, R. M. Stoltenberg, C. V. H.-H. Chen, S. Barman, B. V. O. Muir, A. N. Sokolov, C. Reese, and Z. Bao, Nat. Mater. **9**, 859 (2010).
[4]T. Someya, T. Sekitani, S. Iba, Y. Kato, H. Kawaguchi, and T. Sakurai, Proc. Natl. Acad. Sci. U.S.A. **101**, 9966 (2004).
[5]D.-H. Kim, N. Lu, R. Ghaffari, and J. A. Rogers, NPG Asia Mater. **4**, e15 (2012).
[6]A. Kumar and C. Zhou, ACS Nano **4**, 11 (2010).
[7]K. Ellmer, Nat. Photonics **6**, 809 (2012).
[8]T.-H. Han, Y. Lee, M.-R. Choi, S.-H. Woo, S.-H. Bae, B. H. Hong, J.-H. Ahn, and T.-W. Lee, Nat. Photonics **6**, 105 (2012).
[9]Z. Wu, Z. Chen, X. Du, J. M. Logan, J. Sippel, M. Nikolou, K. Kamaras, J. R. Reynolds, D. B. Tanner, A. F. Hebard, and A. G. Rinzler, Science **305**, 1273 (2004).
[10]K. Fehse, K. Walzer, K. Leo, W. Lövenich, and A. Elschner, Adv. Mater. **19**, 441 (2007).

[11]W. Gaynor, S. Hofmann, M. G. Christoforo, C. Sachse, S. Mehra, A. Salleo, M. D. McGehee, M. C. Gather, B. Lüssem, L. Müller-Meskamp, P. Peumans, and K. Leo, Adv. Mater. **25**, 4006 (2013).
[12]L. Li, J. Liang, S.-Y. Chou, X. Zhu, X. Niu, Z. Yu, and Q. Pei, Sci. Rep. **4**, 4307 (2014).
[13]J. Meyer, P. R. Kidambi, B. C. Bayer, C. Weijtens, A. Kuhn, A. Centeno, A. Pesquera, A. Zurutuza, J. Robertson, and S. Hofmann, Sci. Rep. **4**, 5380 (2014).
[14]S. Hofmann, M. Thomschke, B. Lüssem, and K. Leo, Opt. Express **19**, A1250 (2011).
[15]S. Hofmann, M. Thomschke, P. Freitag, M. Furno, B. Luüssem, and K. Leo, Appl. Phys. Lett. **97**, 253308 (2010).
[16]M. Thomschke, R. Nitsche, M. Furno, and K. Leo, Appl. Phys. Lett. **94**, 083303 (2009).
[17]S. Reineke, M. Thomschke, B. Lüssem, and K. Leo, Rev. Mod. Phys. **85**, 1245 (2013).
[18]M. C. Gather and S. Reineke, J. Photonics Energy **5**, 057607 (2015).
[19]T. Schwab, S. Schubert, L. Müller-Meskamp, K. Leo, and M. C. Gather, Adv. Opt. Mater. **1**, 921 (2013).
[20]T. Schwab, S. Schubert, S. Hofmann, M. Fröbel, C. Fuchs, M. Thomschke, L. Müller-Meskamp, K. Leo, and M. C. Gather, Adv. Opt. Mater. **1**, 707 (2013).
[21]S. Schubert, J. Meiss, L. Müller-Meskamp, and K. Leo, Adv. Energy Mater. **3**, 438 (2013).
[22]G. Schwartz, K. Fehse, M. Pfeiffer, K. Walzer, and K. Leo, Appl. Phys. Lett. **89**, 083509 (2006).
[23]See supplementary material at http://dx.doi.org/10.1063/1.4934274 for profilometer scans, spectrally resolved angular dependent emission, simulated CIE shifts, and device lifetime data.
[24]R. Meerheim, R. Nitsche, and K. Leo, Appl. Phys. Lett. **93**, 043310 (2008).
[25]P. Freitag, S. Reineke, S. Olthof, M. Furno, B. Lüssem, and K. Leo, Org. Electron. **11**, 1676 (2010).
[26]S. Hofmann, T. Schwab, F. Fries, M. Fröbel, S. Schubert, L. Müller-Meskamp, K. Leo, M. C. Gather, and S. Reineke, in Conference on Solid-State and Organic Lighting, 2014.